ACS Photonics

pubs.acs.org/journal/apchd5 Article

Four-Dimensional Printing of a Fiber-Tip Multimaterial Microcantilever as a Magnetic Field Sensor

Haoqiang Huang, Changrui Liao,* Mengqiang Zou, Dejun Liu, Shen Liu, Ying Wang, Zhiyong Bai, Dan Liu, Bozhe Li, Jiabin Huang, Famei Wang, Jie Zhou, Cong Zhao, Xiaoyu Weng, Liwei Liu, Junle Qu, and Yiping Wang

Cite This: *ACS Photonics* 2023, 10, 1916−1924 Read Online

ABSTRACT: "Lab on Fiber" technology integrates different micro- and nanoscale structures or materials onto optical fibers to create additional functionality. With the advanced femtosecond (Fs) laser-induced two-photon polymerization (TPP) technology, polymer microstructures printed on a fiber tip have great potential as micro-optical sensors. However, additional functionalization is usually required, which is costly and complex. Based on the advanced four-dimensional (4D) printing theory, for the first time, a successive multimaterial on-fiber TPP strategy is proposed here, and a fiber-tip polymer microcantilever-based magnetic sensor is prepared in one step. First, the cantilever and the supporting base on the fiber tip are printed by TPP, and then the magnetically responsive cube on the cantilever tip is printed with a self-made magnetic fluid photoresist. The whole process is completed in one step without additional treatment. The prepared sensor shows a minuscule size and a high magnetic sensitivity of 119 pm mT^{-1} in the range of 0−90 mT, suitable for weak or microspace magnetic field measurement at high spatial resolution. Especially, the proposed 4D successive on-fiber TPP strategy can be extended to other stimulus-responsive materials, providing new guidance for manufacturing various stimulus-responsive microsensors and microactuators on the fiber tip.

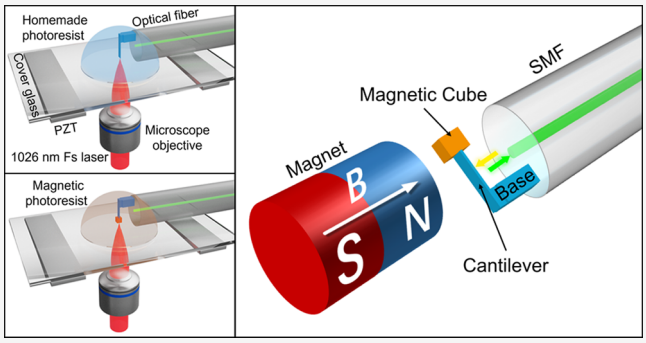

KEYWORDS: *4D printing, successive on-fiber fabrication, optical fiber sensor, magnetic sensor, microcantilever, two-photon polymerization*

■ INTRODUCTION

Magnetic sensors are widely used in power systems,[1,2] magnetic navigation,[3] space science,[4] controllable nuclear fusion,[5] mineral exploration,[6] medical diagnosis,[7−9] and other fields.[10,11] With the "Lab on Fiber" technology developing further, optical fiber sensors have been widely applied in magnetic sensing[12,13] due to their immunity to electromagnetic interference, miniaturized structure, high sensitivity, quick response, and the potential for remote sensing.[14] The optical fiber end facets are inherently extensible platforms for multifarious micro- and nano-optical sensing structures.[15−22] Femtosecond (Fs) laser-induced two-photon polymerization (TPP) is a three-dimensional (3D) printing technology with nanometer resolution, widely used to print polymer micro- and nanostructures of an arbitrary shape.[15,23−31] With the advantages of high integration and short response time, the fiber-tip polymer microcantilever sensors have been widely used for highly sensitive measurement of microforce,[23,32] hydrogen,[33,34] organic solvent,[15] and microfluid.[35] After being functionalized with magnetically responsive materials, the fiber-tip polymer microcantilever is expected as a highly sensitive magnetic sensor. However, traditional treatments such as electron beam sputtering and chemical coating cannot achieve precise functionalization of a local microstructure and require additional postprocessing, which limits its further application.[36−39] Four-dimensional (4D) printing is a process where 3D-printed objects autonomously change their configuration or function in response to environmental stimuli, such as exposure to heat, magnetic field, light, liquid, gas, and prestress.[40,41]

Here, we report a successive multimaterial on-fiber TPP strategy for 4D microstructure fabrication and prepare a fiber-tip polymer magnetic sensing microcantilever in one step. First, the polymer cantilever beam and the supporting base are printed by Fs-laser-induced TPP on the end facet of a single-mode fiber (SMF). Then, the magnetic photoresist containing

Received: March 14, 2023
Published: May 18, 2023

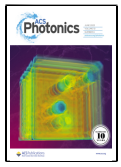

https://doi.org/10.1021/acsphotonics.3c00347
ACS Photonics 2023, 10, 1916−1924

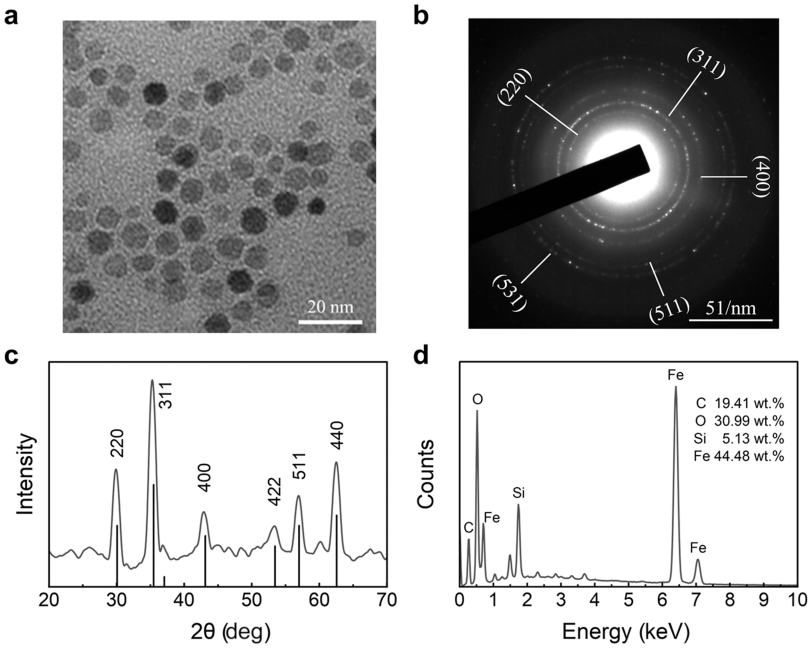

Figure 1. Characterization of MPS−Fe_3O_4 nanoparticles. (a) TEM image of the synthesized MPS−Fe_3O_4 nanoparticles. (b) SAED pattern of a single MPS−Fe_3O_4 nanoparticle. (c) XRD pattern of MPS−Fe_3O_4 nanoparticles at 300 K; bottom: JCPDS card (007-0322) data for magnetite. (d) EDS spectrum of MPS−Fe_3O_4 nanoparticles.

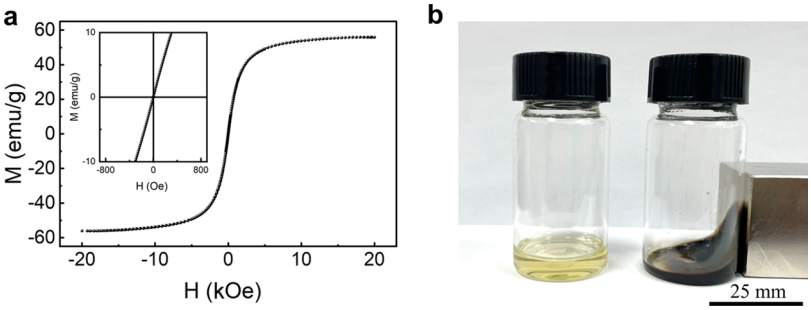

Figure 2. Magnetic property characterization. (a) Hysteresis curve of MPS−Fe_3O_4 nanoparticles. (b) Images of the photoresist before and after doping with MPS−Fe_3O_4 nanoparticles.

Fe_3O_4 nanoparticles is employed to print a magnetically responsive cube at the cantilever tip. The light traveling in the SMF is successively reflected at the fiber end facet and the cantilever, producing a Fabry−Perot interference (FPI) signal. The magnetic cube is attracted by the magnetic field, which makes the cantilever beam bend and results in the FPI cavity length changing. The cantilever beam deformation is tracked by the dip wavelength in the reflection spectrum. A high sensitivity of 119 pm mT^{-1} is realized for the microcantilever magnetic sensor with a test range of 0−90 mT, better than other optical fiber sensors based on magnetic deformation.[42] The miniaturized structure endows the sensor with the capacity of high spatial resolution magnetic sensing. Significantly, the successive multimaterial on-fiber TPP strategy is also applicable to process other stimulus-responsive materials. Therefore, fiber-tip microsensors or microactuators responding to light, heat, electric field, magnetic field, gas, and liquid could be developed. Such a strategy provides an innovative direction for the further development of advanced optical fiber sensors.

RESULTS AND DISCUSSION

Material Characterization. With developed Fs-laser-induced TPP technology, the magnetic photoresist doped with superparamagnetic Fe_3O_4 nanoparticles has been widely used for printing magnetic microstructures with an arbitrary shape.[43,44] The absence of remanence and coercive force endows the printed microstructure with a fast magnetic response and good repeatability.[45] First, Fe_3O_4 nanoparticles coated with oleic acid are synthesized according to the reported method.[46] Then, the surfactant methacryloxy propyl trimethoxy silane (MPS) is employed to modify the synthesized nanoparticles for good dispersibility and photopolymerization. The transmission electron microscopy (TEM) image (Figure 1a) shows that MPS−Fe_3O_4 nanoparticles have a spherical shape with a diameter of 6 nm. The high-resolution TEM (HRTEM) image clearly illustrates that the nanoparticles are cubic Fe_3O_4, as shown in Figure S1; the lattice fringes with a distance of 2.96 Å ascribe well to the (220) planes of Fe_3O_4. Figure 1b shows the selected area electron diffraction (SAED) pattern from a single MPS−Fe_3O_4 nanoparticle, and the homogeneous ring patterns are consistent with the lattice spacings of Fe_3O_4. Besides, the X-ray diffraction (XRD)

https://doi.org/10.1021/acsphotonics.3c00347
ACS Photonics 2023, 10, 1916−1924

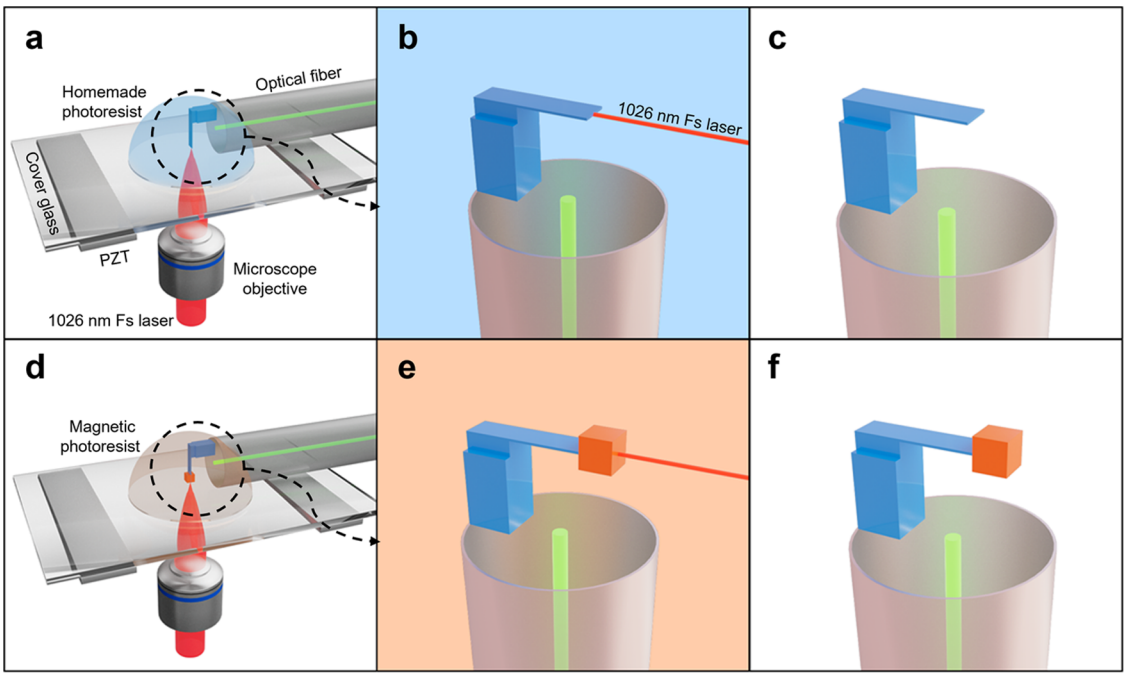

Figure 3. Schematic diagram of the successive multimaterial TPP printed magnetic microcantilever on the fiber end facet. (a) Fiber tip is immersed in the original photoresist, and a cover glass is employed to keep the oil separate from the photoresist and protect the objective lens. (b) TPP fabrication of the microcantilever. (c) Developed microcantilever after removing the unexposed photoresist. (d) Secondary integration via TPP. (e) TPP fabrication of the magnetic cube at the cantilever tip. (f) Magnetic cube-modified fiber-tip microcantilever after development.

pattern (Figure 1c) shows several diffraction peaks of the synthesized MPS−Fe_3O_4 nanoparticles, which correspond to the 220, 311, 400, 422, 511, and 440 planes of cubic inverse spinel, consistent with the standard pattern of Fe_3O_4 from the JCPDS card (no. 007-0322).[46] As shown in Figure 1d, the energy-dispersive spectrometry (EDS) analysis proves the presence of the elements C, O, Fe, and Si in MPS−Fe_3O_4 nanoparticles, giving strong evidence for the successful grafting of MPS groups.

Before TPP processing, the magnetic property of MPS−Fe_3O_4 nanoparticles and a magnetic fluid photoresist are studied. The physical property measurement system is employed to analyze the magnetic properties of MPS−Fe_3O_4 nanoparticles at 300 K, and the result (Figure 2a) shows no remanence and coercive force, indicating it is superparamagnetic. The saturation magnetization of nanoparticles is ∼55 emu g^{-1} at 300 K, which provides a sufficient magnetic response. To obtain the magnetic fluid photoresist, 2 wt % MPS−Fe_3O_4 nanoparticles are homogeneously mixed into a preprepared photoresist, which comprises a photoinitiator (2-benzyl-2-(dimethylamino)-4′-morpholino-butyroph (IGR-369)), an inhibitor (4-hydroxyanisole (MEHQ)), and three acrylate monomers (pentaerythritol triacrylate (PETA), tris(2-(acryloyloxy)ethyl)isocyanurate (THEICTA) and trimethylolpropane ethoxylate triacrylate (TMPEOTA)). The clever combination of these three monomers ensures the structural strength and no shrinkage during polymerization. As shown in Figure 2b, the photoresist before doping appears transparent and clear. After being doped with MPS−Fe_3O_4 nanoparticles, the photoresist presents a brown-black translucent liquid with a uniform texture. Even under the attraction of a permanent magnet, no magnetic nanoparticles separate from the resin carrier, indicating a stable colloidal dispersion consisting of the MPS−Fe_3O_4 and the photoresist, namely ferrofluid. Herein, the MPS ligand on the surface of nanoparticles has a similar structure and polarity to acrylate, which endows this organic/inorganic mixed system with a good dispersion and photopolymerizable feature, which will contribute to the following laser processing.

Successive Multimaterial On-Fiber TPP Strategy. To endow a 3D microstructure with stimulus-responsive characteristics, additional functional processing is necessary. However, the traditional treatment, such as electron beam sputtering and chemical coating, requires additional post-processing and cannot achieve precise functionalization of the local microstructure.[36,37,39] Based on the advanced 4D printing theory, here we show a successive multimaterial on-fiber TPP strategy and realize one-step fabrication of a fiber-tip polymer microcantilever magnetic sensor. First, with a homemade photoresist, the polymer microcantilever beam and the supporting base are printed using Fs-laser-induced TPP on the end facet of SMF. The detailed process includes a cleaved SMF (Corning, SMF-28) with an 8/125 μm core/cladding diameter first placed on the glass slide. Then, 50 μL of a self-made photoresist is dropped on the fiber tip carefully before being covered with a cover glass. As shown in Figure 3a, the sample is placed on the 3D translation stage (Aerotech, ANT130V-5) before the laser process. An Fs laser with a 250 fs pulse width, a 1026 nm central wavelength, and a 200 kHz pulse repetition rate is employed in the polymerization process. The laser beam is focused by a 63× oil-immersion objective lens (Carl Zeiss, NA = 1.4). The laser power before the lens is set to 2 mW, and a scanning speed of 0.5 mm s^{-1} is employed after optimization. The schematic diagram of our TPP printing system is shown in Figure S2. As shown in Figure 3b, the cantilever is printed on the fiber tip according to a preprogrammed model. After polymerization, the optical fiber is carefully taken off and immersed in a mixed solvent of isopropyl alcohol and acetone (volume ratio = 3:1) for 3 min to remove the unreacted photoresist. The well-printed

https://doi.org/10.1021/acsphotonics.3c00347
ACS Photonics 2023, 10, 1916−1924

microcantilever on the fiber tip is shown in Figure 3c. Subsequently, with a magnetic photoresist containing Fe_3O_4 nanoparticles, a magnetically responsive cube is printed on the cantilever tip. The details are as follows: First, the developed fiber sample was placed on a new slide. Then, 50 μL of a magnetic photoresist was dropped on the fiber tip before placing the cover glass above (Figure 3d). All laser parameters remained unchanged, but the laser power was set to 4 mW. After the second printing, a 20 μm magnetic cube was printed on the cantilever tip (Figure 3e). After development for 5 min, the well-made fiber-tip microcantilever modified with a magnetic cube was finished, as shown in Figure 3f.

Sensor Characterization and the Principle. Figure 4a,b shows the false-color scanning electron microscopy (SEM) images of the polymeric magnetic microcantilever from the top view and the side view. The whole microstructure is composed of three parts, a supporting base, a cantilever beam, and a magnetic cube. The base is ~50 μm high, with a 20 × 30 μm^2 of cross-sectional area to make reliable contact with the optical fiber end facet. The top of the base is attached to a cantilever beam with a width of 20 μm and a thickness of 3 μm. The length of the cantilever beam is set as 90 μm for a smaller elastic coefficient and higher strain sensitivity. The other end of the cantilever beam is connected to a magnetic photoresist-printed cube with a 20 μm side length. The bigger volume of the magnetic cube ensures a higher sensitivity to a magnetic field. It could be found that the whole printed microstructure has a clear contour and smooth surface, proving the high accuracy of TPP in processing multiple materials. No gap can be seen in the joint of the magnetic cube and the cantilever beam, ensuring the stability of the magnetic sensor. Besides, the good parallelism between the cantilever beam and optical fiber end facet also assures the contrast of the reflection spectrum.

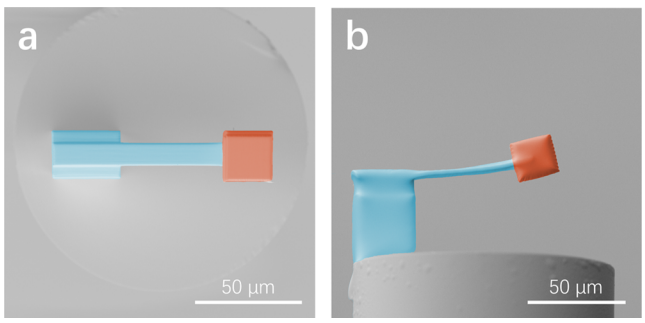

Figure 4. Morphological characterization of the magnetic microcantilever. (a, b) False-color SEM images of the magnetic cube (orange)-modified fiber-tip microcantilever (blue) in various views.

Using an amplified spontaneous emission (ASE) light source with an optical spectrum analyzer (OSA), the reflection spectrum of the microcantilever sensor at a zero-field condition is measured, as shown in Figure 5a. Around 1350 nm, the fringe visibility and free spectral range (FSR) are measured as ~9 dB and ~23 nm, respectively. The interference pattern can be interpreted with a three-beam interference induced by the fiber end facet, the lower and upper surfaces of the cantilever. In fact, three interference cavities are formed total. The first FPI (FPI_1) is the air cavity between the fiber end facet and the cantilever's lower surface, the second FPI (FPI_2) is the polymer cavity between the two surfaces of the cantilever, and the third FPI (FPI_3) is the mixed cavity between the fiber end facet and the cantilever's upper surface. Considering the negligible light intensity of FPI_3 and the fixed cavity length of FPI_2 after manufacturing, here, FPI_1 is selected for demodulation, and its FSR can be calculated by this equation

$$\mathrm{FSR} = \frac{\lambda^2}{2nL} \tag{1}$$

where λ is the dip wavelength, n is the refractive index of the cavity medium, and L is the cavity length.

In this experiment, Fe_3O_4 nanoparticles in the magnetic cube are magnetized by the external magnetic field and thus subjected to magnetic force, resulting in the cantilever beam bending outward (Figure 5b). The cantilever deflection equals the increase of the cavity length. The relationship between the dip wavelength shift ($\Delta\lambda$) and the cavity length increase ($\Delta L = L_2 - L_1$) follows (ref 23)

$$\frac{\Delta\lambda}{\lambda} = \frac{\Delta L}{L} \tag{2}$$

Therefore, the magnetic field intensity can be derived by direct measurement of the dip wavelength shift. When the magnetic sensor is placed in an external static magnetic field, the translation force (F_m) on the magnetic cube can be expressed as follows

$$F_m = \nabla(m \cdot B) \tag{3}$$

Here, m is the dipole moment of the magnetic cube, B is the imposed magnetic field strength, and ∇ is the gradient of the quantity ($m \cdot B$) along the dipole length.[13]

In magnetostatic equilibrium, the magnitude of F_m is equal to that of the microcantilever restitutive force F_z. Therefore,

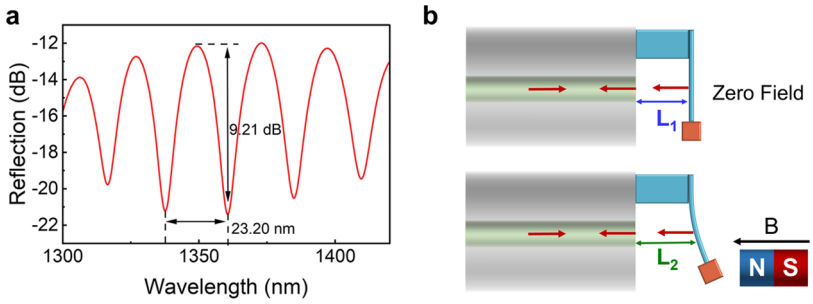

Figure 5. Original spectrum and the sensing principle of the microcantilever sensor. (a) Initial reflected spectrum of the optical fiber sensor at the zero-field condition with a 50 μm cavity length. (b) Working principle of the fiber-tip microcantilever sensor within an external magnetic field, where L_1 and L_2 represent the cantilever cavity length before and after the magnetic field is applied, respectively.

https://doi.org/10.1021/acsphotonics.3c00347
ACS Photonics 2023, 10, 1916−1924

according to Hooke's law $F_z = -k\Delta z$, the cantilever bending is proportional to the force on the magnetic cube and linearly depends on field strength, which can be expressed as the following equation

$$\Delta z = \frac{\nabla(m \cdot B)}{k} \tag{4}$$

Here, the spring coefficient of the cantilever beam can be expressed as $K = 3EI/L^3$, where E is Young's modulus of the cantilever material, I is the second moment of the area of the cantilever beam, and L is the length of the cantilever beam.[47]

Magnetic Sensing Test. The setup for the magnetic sensing test is shown in Figure 6a, where an ASE light source with a range from 1250 to 1650 nm is used to guide the light to the magnetic sensor through the 3 dB coupler, and the reflection spectrum is recorded by using an OSA with a 20 pm minimum resolution. The magnetic field is provided by a zinc-coated NdFeB magnet rod of dimensions 0.1 mm × 1.5 mm fixed on a manual 3D translation stage (Figure 6b). The optical fiber sensor is fixed on a base and kept parallel to the axis of the magnet rod to ensure the maximum magnetic gradient. The translation stage is employed to adjust the distance between the magnetic rod and the sensor. By moving the translation stage, the magnetic flux changes accordingly. A Gauss meter is used to monitor the magnetic field change in real-time. The advantage of using an NdFeB magnet as a magnetic field generator is to avoid electromagnetic coil emitting heat. The whole experiment is conducted at room temperature (25 °C) to avoid the influence of temperature on the measurement result.

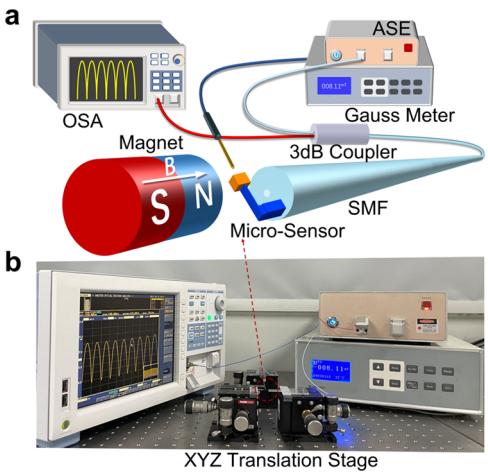

Figure 6. Experiment setup. (a) Schematic of the experimental setup for magnetic field sensing. (b) Photograph of the experimental setup. The magnetic field intensity is adjusted by moving the translation stage.

By moving the translation stage, the magnetic field intensity around the sensor increases from 0 to 90 mT in an increase of 10 mT. The corresponding dip wavelength shift was observed and recorded, and the measurement was repeated three times. The reflection spectrum of the microcantilever in a magnetic field is shown in Figure 7a. It can be found that the reflection spectrum is gradually shifted to the longer wavelength with the magnetic intensity increasing. When the imposed magnetic field intensity increases from 0 to 90 mT, the total dip wavelength shift near 1345 nm is ∼12 nm. The dip wavelength vs magnetic field intensity is plotted in Figure 7b. The result shows that the dip wavelength shift is an approximately linear function of magnetic field strength, with a slope of 0.119 nm mT^{-1} and a fitting confidence of 0.993. The magnetic field measurement accuracy is calculated as 166.7 μT considering the OSA with a 20 pm resolution. The results demonstrate that the magnetic cantilever is deformed under the action of a magnetic field, which affects the length of the FPI cavity and leads to the change of the resonance wavelength.

To test the repeatability and stability of the magnetic field sensor to the magnetic field within the linear range, the experiments are repeatedly performed in three cycles under different magnetic field conditions. During this measurement, the magnetic field first increases from 0 to 90 mT and then decreases to 0 mT in 10 mT steps. The dip wavelength near 1345 nm under different magnetic fields is plotted in Figure 8.

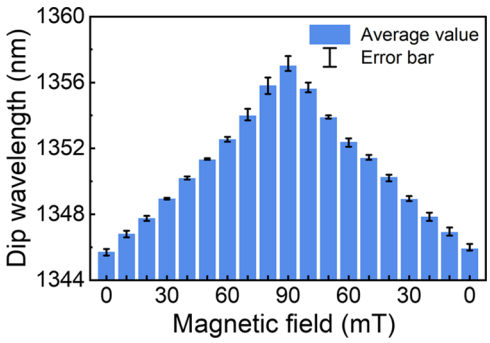

Figure 8. Repeated tests of the dip wavelength under different magnetic fields.

The results show that the dip wavelength is relatively stable to the externally imposed magnetic field no matter whether the

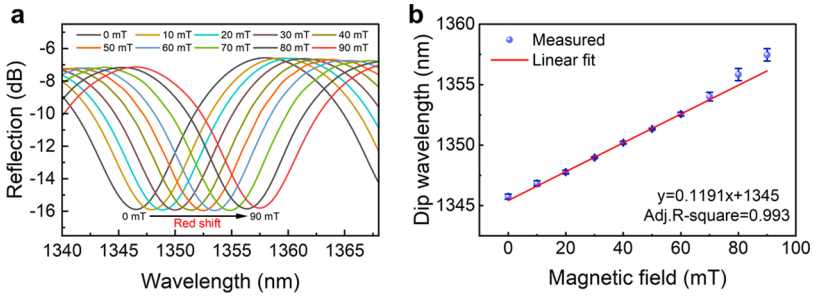

Figure 7. Response of the magnetic sensor to magnetic field intensity. (a) Reflection spectrum of the sensor under different magnetic field intensities. (b) Linear fitting of the dip wavelength against the applied magnetic field.

https://doi.org/10.1021/acsphotonics.3c00347
ACS Photonics 2023, 10, 1916−1924

magnetic field intensity increases or decreases. The response of the microcantilever sensor to the externally applied magnetic field has good repeatability. Compared with other reported magnetic deformation-based magnetic field sensors, the magnetic cantilever has excellent magnetic field sensitivity, a wide measurement range, and high stability.[42]

CONCLUSIONS

Here, we report a successive 4D multimaterial on-fiber TPP strategy for optical microstructure fabrication and prepare a fiber-tip polymer microcantilever magnetic sensor in one step. First, the microcantilever beam and the supporting base are printed on the end facet of an optical fiber with a self-made photoresist. Then, the magnetically responsive photoresist doped with paramagnetic MPS−Fe_3O_4 nanoparticles is employed to print a magnetic cube at the cantilever tip as a magnetically responsive element. The whole manufacturing process is completed in one step, avoiding further postprocessing. The sensitivity of the microcantilever magnetic sensor is up to 119 pm mT^{-1} in the range of 0−90 mT, and the total dip wavelength shift near 1345 nm is ∼12 nm. The stability experiment proves that the sensor has very high repeatability. Compared with the existing commercial magnetic sensor, our sensor supplies an ultracompact optical solution, which effectively avoids the interference of electrical excitation on the measured magnetic field and maintains an extremely small size. It is well suited for weak or microspace magnetic field measurement at high spatial resolution. Significantly, the 4D successive on-fiber TPP strategy that permits the integration of multiform materials into 3D microstructures is universal, not limited to photoresist systems with magnetically responsive materials. With the rapid development of advanced intelligent materials, this strategy will be suitable for preparing 4D optical fiber-tip microsensors and microactuators with various stimulus-responsive characteristics (light, heat, electric field, magnetic field, gas and liquid).

MATERIALS AND METHODS

Materials. $Fe(acac)_3$, 1,2-hexadecanediol, oleic acid, oleylamine, benzyl ether, and methacryloxy propyl trimethoxy silane (MPS) were purchased from Aladdin. Pentaerythritol triacrylate (PETA), tris(2-(acryloyloxy)ethyl)isocyanurate (THEICTA), trimethylolpropane ethoxylate triacrylate (TMPEOTA), 2-benzyl-2-(dimethylamino)-4′-morpholinobutyroph (IGR-369), tetraethyl thiuram disulfide (TED), and 4-hydroxyanisole (MEHQ) were purchased from Sigma-Aldrich.

Synthesis of Fe_3O_4 Nanoparticles. Fe_3O_4 nanoparticles are synthesized according to the reported method in ref 46. In brief, $Fe(acac)_3$ (0.706 g), 1,2-hexadecanediol (2.58 g), oleic acid (1.904 mL), oleylamine (1.974 mL), and benzyl ether (20 mL) were added in a round-bottom flask and stirred in an argon atmosphere (1000 rpm). The temperature of the evenly stirred reaction system was increased to 200 °C for 2 h and then heated to reflux (∼300 °C) for 1 h. Meantime, the solution color changed from brown to black. After the reaction system cooled to room temperature, ethanol (40 mL) was added to precipitated Fe_3O_4 nanoparticles under an argon atmosphere; then, the black precipitation was separated via centrifugation (6000 rpm, 3 min). The product was continuously washed with 40 mL of hexane/ethanol (1:3). After centrifugation (6000 rpm, 3 min) three times, the Fe_3O_4 nanoparticles were redispersed into hexane (10 mL).

Preparation of MPS−Fe_3O_4 Nanoparticles. For further grafting, the Fe_3O_4 nanoparticles (0.46 g) were mixed with toluene (20 mL) in a three-neck flask, and then MPS (0.3 g) was added under Ar protection. The reaction system was kept stirring at 50 °C for 24 h. Then, the product was centrifuged (6000 rpm, 3 min) and washed with ethanol three times, giving MPS−Fe_3O_4 nanoparticles.

Preparation of an Original Photoresist and a Magnetic Photoresist. A homemade photoresist is prepared by mixing 40 wt % PETA, 30 wt % THEICTA, 25 wt % TMPEOTA, 2.5 wt % IGR-369, and 2 wt % TED with 0.5 wt % MEHQ. The magnetic photoresist was prepared by adding the synthesized MPS−Fe_3O_4 nanoparticles (2 wt %) into the homemade photoresist with full ultrasound mixing.

Characterization. Transmission electron microscopy (TEM) images of Fe_3O_4 nanoparticles were derived from a transmission electron microscope (HT7700, Hitachi). In detail, 10 μL of a Fe_3O_4 nanoparticle suspension was dropped on a TEM grid. After dying, the grid was observed under a TEM with a 200 kV accelerative voltage. The XRD pattern was obtained by using a high-resolution X-ray diffractometer (X′pert pro, Philips) with Cu Kα radiation at a 20−80° measuring range and a 2° min^{-1} scanning speed. Magnetic measurements were obtained from a Physical Property Measurement System (DynaCool, Quantum Design). High-resolution TEM (HRTEM) spectroscopy, selected area electron diffraction (SAED), and energy-dispersive X-ray spectroscopy (EDS) were performed by an HRTEM (JEM-F200, JEOL).

ASSOCIATED CONTENT

Supporting Information

The Supporting Information is available free of charge at https://pubs.acs.org/doi/10.1021/acsphotonics.3c00347.

HRTEM image of MPS−Fe_3O_4 nanoparticles and the schematic diagram of our TPP printing system (PDF)

AUTHOR INFORMATION

Corresponding Author

Changrui Liao − *Shenzhen Key Laboratory of Photonic Devices and Sensing Systems for Internet of Things, Guangdong and Hong Kong Joint Research Centre for Optical Fibre Sensors, State Key Laboratory of Radio Frequency Heterogeneous Integration, Shenzhen University, Shenzhen 518060, China; Shenzhen Key Laboratory of Ultrafast Laser Micro/Nano Manufacturing, Key Laboratory of Optoelectronic Devices and Systems of Ministry of Education/Guangdong Province, College of Physics and Optoelectronic Engineering, Shenzhen University, Shenzhen 518060, China;* orcid.org/0000-0003-3669-5054; Email: cliao@szu.edu.cn

Authors

Haoqiang Huang − *Shenzhen Key Laboratory of Photonic Devices and Sensing Systems for Internet of Things, Guangdong and Hong Kong Joint Research Centre for Optical Fibre Sensors, State Key Laboratory of Radio Frequency Heterogeneous Integration, Shenzhen University, Shenzhen 518060, China; Shenzhen Key Laboratory of Ultrafast Laser Micro/Nano Manufacturing, Key Laboratory*

of Optoelectronic Devices and Systems of Ministry of Education/Guangdong Province, College of Physics and Optoelectronic Engineering, Shenzhen University, Shenzhen 518060, China

Mengqiang Zou − *Shenzhen Key Laboratory of Photonic Devices and Sensing Systems for Internet of Things, Guangdong and Hong Kong Joint Research Centre for Optical Fibre Sensors, State Key Laboratory of Radio Frequency Heterogeneous Integration, Shenzhen University, Shenzhen 518060, China; Shenzhen Key Laboratory of Ultrafast Laser Micro/Nano Manufacturing, Key Laboratory of Optoelectronic Devices and Systems of Ministry of Education/Guangdong Province, College of Physics and Optoelectronic Engineering, Shenzhen University, Shenzhen 518060, China*

Dejun Liu − *Shenzhen Key Laboratory of Photonic Devices and Sensing Systems for Internet of Things, Guangdong and Hong Kong Joint Research Centre for Optical Fibre Sensors, State Key Laboratory of Radio Frequency Heterogeneous Integration, Shenzhen University, Shenzhen 518060, China; Shenzhen Key Laboratory of Ultrafast Laser Micro/Nano Manufacturing, Key Laboratory of Optoelectronic Devices and Systems of Ministry of Education/Guangdong Province, College of Physics and Optoelectronic Engineering, Shenzhen University, Shenzhen 518060, China*

Shen Liu − *Shenzhen Key Laboratory of Photonic Devices and Sensing Systems for Internet of Things, Guangdong and Hong Kong Joint Research Centre for Optical Fibre Sensors, State Key Laboratory of Radio Frequency Heterogeneous Integration, Shenzhen University, Shenzhen 518060, China; Shenzhen Key Laboratory of Ultrafast Laser Micro/Nano Manufacturing, Key Laboratory of Optoelectronic Devices and Systems of Ministry of Education/Guangdong Province, College of Physics and Optoelectronic Engineering, Shenzhen University, Shenzhen 518060, China;* orcid.org/0000-0001-9266-2498

Ying Wang − *Shenzhen Key Laboratory of Photonic Devices and Sensing Systems for Internet of Things, Guangdong and Hong Kong Joint Research Centre for Optical Fibre Sensors, State Key Laboratory of Radio Frequency Heterogeneous Integration, Shenzhen University, Shenzhen 518060, China; Shenzhen Key Laboratory of Ultrafast Laser Micro/Nano Manufacturing, Key Laboratory of Optoelectronic Devices and Systems of Ministry of Education/Guangdong Province, College of Physics and Optoelectronic Engineering, Shenzhen University, Shenzhen 518060, China;* orcid.org/0000-0001-8020-3622

Zhiyong Bai − *Shenzhen Key Laboratory of Photonic Devices and Sensing Systems for Internet of Things, Guangdong and Hong Kong Joint Research Centre for Optical Fibre Sensors, State Key Laboratory of Radio Frequency Heterogeneous Integration, Shenzhen University, Shenzhen 518060, China; Shenzhen Key Laboratory of Ultrafast Laser Micro/Nano Manufacturing, Key Laboratory of Optoelectronic Devices and Systems of Ministry of Education/Guangdong Province, College of Physics and Optoelectronic Engineering, Shenzhen University, Shenzhen 518060, China;* orcid.org/0000-0002-0915-751X

Dan Liu − *Shenzhen Key Laboratory of Photonic Devices and Sensing Systems for Internet of Things, Guangdong and Hong Kong Joint Research Centre for Optical Fibre Sensors, State Key Laboratory of Radio Frequency Heterogeneous Integration, Shenzhen University, Shenzhen 518060, China; Shenzhen Key Laboratory of Ultrafast Laser Micro/Nano Manufacturing, Key Laboratory of Optoelectronic Devices and Systems of Ministry of Education/Guangdong Province, College of Physics and Optoelectronic Engineering, Shenzhen University, Shenzhen 518060, China*

Bozhe Li − *Shenzhen Key Laboratory of Photonic Devices and Sensing Systems for Internet of Things, Guangdong and Hong Kong Joint Research Centre for Optical Fibre Sensors, State Key Laboratory of Radio Frequency Heterogeneous Integration, Shenzhen University, Shenzhen 518060, China; Shenzhen Key Laboratory of Ultrafast Laser Micro/Nano Manufacturing, Key Laboratory of Optoelectronic Devices and Systems of Ministry of Education/Guangdong Province, College of Physics and Optoelectronic Engineering, Shenzhen University, Shenzhen 518060, China*

Jiabin Huang − *Shenzhen Key Laboratory of Photonic Devices and Sensing Systems for Internet of Things, Guangdong and Hong Kong Joint Research Centre for Optical Fibre Sensors, State Key Laboratory of Radio Frequency Heterogeneous Integration, Shenzhen University, Shenzhen 518060, China; Shenzhen Key Laboratory of Ultrafast Laser Micro/Nano Manufacturing, Key Laboratory of Optoelectronic Devices and Systems of Ministry of Education/Guangdong Province, College of Physics and Optoelectronic Engineering, Shenzhen University, Shenzhen 518060, China*

Famei Wang − *Shenzhen Key Laboratory of Photonic Devices and Sensing Systems for Internet of Things, Guangdong and Hong Kong Joint Research Centre for Optical Fibre Sensors, State Key Laboratory of Radio Frequency Heterogeneous Integration, Shenzhen University, Shenzhen 518060, China; Shenzhen Key Laboratory of Ultrafast Laser Micro/Nano Manufacturing, Key Laboratory of Optoelectronic Devices and Systems of Ministry of Education/Guangdong Province, College of Physics and Optoelectronic Engineering, Shenzhen University, Shenzhen 518060, China*

Jie Zhou − *Shenzhen Key Laboratory of Photonic Devices and Sensing Systems for Internet of Things, Guangdong and Hong Kong Joint Research Centre for Optical Fibre Sensors, State Key Laboratory of Radio Frequency Heterogeneous Integration, Shenzhen University, Shenzhen 518060, China; Shenzhen Key Laboratory of Ultrafast Laser Micro/Nano Manufacturing, Key Laboratory of Optoelectronic Devices and Systems of Ministry of Education/Guangdong Province, College of Physics and Optoelectronic Engineering, Shenzhen University, Shenzhen 518060, China*

Cong Zhao − *Guangdong Laboratory of Artificial Intelligence and Digital Economy (SZ), Shenzhen 518107, China*

Xiaoyu Weng − *Shenzhen Key Laboratory of Ultrafast Laser Micro/Nano Manufacturing, Key Laboratory of Optoelectronic Devices and Systems of Ministry of Education/Guangdong Province, College of Physics and Optoelectronic Engineering, Shenzhen University, Shenzhen 518060, China*

Liwei Liu − *Shenzhen Key Laboratory of Ultrafast Laser Micro/Nano Manufacturing, Key Laboratory of Optoelectronic Devices and Systems of Ministry of Education/Guangdong Province, College of Physics and Optoelectronic Engineering, Shenzhen University, Shenzhen 518060, China;* orcid.org/0000-0002-4593-665X

Junle Qu − *Shenzhen Key Laboratory of Ultrafast Laser Micro/Nano Manufacturing, Key Laboratory of Optoelectronic Devices and Systems of Ministry of Education/Guangdong Province, College of Physics and Optoelectronic Engineering, Shenzhen University, Shenzhen 518060, China*

https://doi.org/10.1021/acsphotonics.3c00347
ACS Photonics 2023, 10, 1916−1924

Yiping Wang − *Shenzhen Key Laboratory of Photonic Devices and Sensing Systems for Internet of Things, Guangdong and Hong Kong Joint Research Centre for Optical Fibre Sensors, State Key Laboratory of Radio Frequency Heterogeneous Integration, Shenzhen University, Shenzhen 518060, China; Shenzhen Key Laboratory of Ultrafast Laser Micro/Nano Manufacturing, Key Laboratory of Optoelectronic Devices and Systems of Ministry of Education/Guangdong Province, College of Physics and Optoelectronic Engineering, Shenzhen University, Shenzhen 518060, China; Guangdong Laboratory of Artificial Intelligence and Digital Economy (SZ), Shenzhen 518107, China*

Complete contact information is available at: https://pubs.acs.org/10.1021/acsphotonics.3c00347

Author Contributions

Haoqiang Huang and Changrui Liao jointly conceived the idea. Haoqiang Huang and Changrui Liao designed and fabricated the devices, built the experimental setup, and carried out the experiments. Haoqiang Huang, Mengqiang Zou, Dan Liu, Bozhe Li, Jiabin Huang, Famei Wang, Jie Zhou, and Cong Zhao analyzed the data. Dejun Liu, Shen Liu, Ying Wang, Zhiyong Bai, Xiaoyu Weng, Liwei Liu, Junle Qu, and Yiping Wang assisted with the theory. Haoqiang Huang and Changrui Liao wrote the manuscript with contributions from all co-authors. All authors have given approval to the final version of the manuscript.

Funding

This work was supported by the National Natural Science Foundation of China (62122057, 62075136, 62105217), the Natural Science Foundation of Guangdong Province (2022B1515120061), and the Science and Technology Innovation Commission of Shenzhen (RCYX20200714114524139, JCYJ20200109114001806, JCYJ20190808173401660).

Notes

The authors declare no competing financial interest.

■ REFERENCES

(1) Hu, L.; Wu, H.; Zhang, Q.; You, H.; Jiao, J.; Luo, H.; Wang, Y.; Gao, A.; Duan, C. Self-powered energy-harvesting magnetic field sensor. *Appl. Phys. Lett.* **2022**, *120*, No. 043902.

(2) Su, W.; Wang, Z.; Chen, Y.; Zhao, X.; Hu, C.; Wen, T.; Hu, Z.; Wu, J.; Zhou, Z.; Liu, M. Reconfigurable Magnetoresistive Sensor Based on Magnetoelectric Coupling. *Adv. Electron. Mater.* **2020**, *6*, No. 1901061.

(3) Liakopoulos, T. M.; Ahn, C. H. A micro-fluxgate magnetic sensor using micromachined planar solenoid coils. *Sens. Actuators, A* **1999**, *77*, 66−72.

(4) Wu, J.; Hu, Z.; Gao, X.; Cheng, M.; Zhao, X.; Su, W.; Wang, Z.; Zhou, Z.; Dong, S.; Liu, M. A Magnetoelectric Compass for In-Plane AC Magnetic Field Detection. *IEEE Trans. Ind. Electron.* **2021**, *68*, 3527−3536.

(5) Bolshakova, I.; Bulavin, M.; Kargin, N.; Kost, Y.; Kuech, T.; Kulikov, S.; Radishevskiy, M.; Shurygin, F.; Strikhanov, M.; Vasil'evskii, I.; Vasyliev, A. Metal Hall sensors for the new generation fusion reactors of DEMO scale. *Nucl. Fusion* **2017**, *57*, No. 116042.

(6) Wang, T.; Guo, L.; Lei, C.; Zhou, Y. Detection of the magnetite by giant magnetoimpedance sensor. *Mater. Lett.* **2015**, *158*, 155−158.

(7) Christopher deCharms, R. Applications of real-time fMRI. *Nat. Rev. Neurosci.* **2008**, *9*, 720−729.

(8) Kim, D.-H.; Lu, N.; Ghaffari, R.; Kim, Y.-S.; Lee, S. P.; Xu, L.; Wu, J.; Kim, R.-H.; Song, J.; Liu, Z.; Viventi, J.; de Graff, B.; Elolampi, B.; Mansour, M.; Slepian, M. J.; Hwang, S.; Moss, J. D.; Won, S.-M.; Huang, Y.; Litt, B.; Rogers, J. A. Materials for multifunctional balloon catheters with capabilities in cardiac electrophysiological mapping and ablation therapy. *Nat. Mater.* **2011**, *10*, 316−323.

(9) Karnaushenko, D.; Ibarlucea, B.; Lee, S.; Lin, G.; Baraban, L.; Pregl, S.; Melzer, M.; Makarov, D.; Weber, W. M.; Mikolajick, T.; Schmidt, O. G.; Cuniberti, G. Light Weight and Flexible High-Performance Diagnostic Platform. *Adv. Healthcare Mater.* **2015**, *4*, 1517−1525.

(10) Su, W.; Hu, Z.; Li, Y.; Han, Y.; Chen, Y.; Wang, C.; Jiang, Z.; He, Z.; Wu, J.; Zhou, Z.; Wang, Z.; Liu, M. Easy-Cone Magnetic State Induced Ultrahigh Sensitivity and Low Driving Current in Spin-Orbit Coupling 3D Magnetic Sensors. *Adv. Funct. Mater.* **2022**, *33*, No. 2211752.

(11) Li, Z.; Liao, C.; Song, J.; Wang, Y.; Zhu, F.; Wang, Y.; Dong, X. Ultrasensitive magnetic field sensor based on an in-fiber Mach-Zehnder interferometer with a magnetic fluid component. *Photonics Res.* **2016**, *4*, 197−201.

(12) Pinet, É. Saving lives. *Nat. Photonics* **2008**, *2*, 150−152.

(13) Chatterjee, K.; Pal, S. K.; Jha, R. Reconfigurable Optical Magnetometer for Static and Dynamic Fields. *Adv. Opt. Mater.* **2021**, *9*, No. 2001574.

(14) Yao, Q.; Ren, G.; Xu, K.; Zhu, L.; Khan, H.; Mohiuddin, M.; Khan, M. W.; Zhang, B. Y.; Jannat, A.; Haque, F.; Reza, S. Z.; Wang, Y.; Wen, X.; Mitchell, A.; Ou, J. Z. 2D Plasmonic Tungsten Oxide Enabled Ultrasensitive Fiber Optics Gas Sensor. *Adv. Opt. Mater.* **2019**, *7*, No. 1901383.

(15) Zhang, S.; Tang, S.-J.; Feng, S.; Xiao, Y.-F.; Cui, W.; Wang, X.; Sun, W.; Ye, J.; Han, P.; Zhang, X.; Zhang, Y. High-Q Polymer Microcavities Integrated on a Multicore Fiber Facet for Vapor Sensing. *Adv. Opt. Mater.* **2019**, *7*, No. 1900602.

(16) Kostovski, G.; Stoddart, P. R.; Mitchell, A. The Optical Fiber Tip: An Inherently Light-Coupled Microscopic Platform for Micro- and Nanotechnologies. *Adv. Mater.* **2014**, *26*, 3798−3820.

(17) Ricciardi, A.; Consales, M.; Quero, G.; Crescitelli, A.; Esposito, E.; Cusano, A. Versatile Optical Fiber Nanoprobes: From Plasmonic Biosensors to Polarization-Sensitive Devices. *ACS Photonics* **2014**, *1*, 69−78.

(18) Consales, M.; Ricciardi, A.; Crescitelli, A.; Esposito, E.; Cutolo, A.; Cusano, A. Lab-on-Fiber Technology: Toward Multifunctional Optical Nanoprobes. *ACS Nano* **2012**, *6*, 3163−3170.

(19) Vaiano, P.; Carotenuto, B.; Pisco, M.; Ricciardi, A.; Quero, G.; Consales, M.; Crescitelli, A.; Esposito, E.; Cusano, A. Lab on Fiber Technology for biological sensing applications. *Laser Photonics Rev.* **2016**, *10*, 922−961.

(20) Ricciardi, A.; Consales, M.; Quero, G.; Crescitelli, A.; Esposito, E.; Cusano, A. Lab-on-Fiber devices as an all around platform for sensing. *Opt. Fiber Technol.* **2013**, *19*, 772−784.

(21) Liu, S.; Chen, Y.; Lai, H.; Zou, M.; Xiao, H.; Chen, P.; Du, B.; Xiao, X.; He, J.; Wang, Y. Room-Temperature Fiber Tip Nanoscale Optomechanical Bolometer. *ACS Photonics* **2022**, *9*, 1586−1593.

(22) Giaquinto, M.; Aliberti, A.; Micco, A.; Gambino, F.; Ruvo, M.; Ricciardi, A.; Cusano, A. Cavity-Enhanced Lab-on-Fiber Technology: Toward Advanced Biosensors and Nano-Opto-Mechanical Active Devices. *ACS Photonics* **2019**, *6*, 3271−3280.

(23) Zou, M.; Liao, C.; Liu, S.; Xiong, C.; Zhao, C.; Zhao, J.; Gan, Z.; Chen, Y.; Yang, K.; Liu, D.; Wang, Y.; Wang, Y. Fiber-tip polymer clamped-beam probe for high-sensitivity nanoforce measurements. *Light: Sci. Appl.* **2021**, *10*, No. 171.

(24) Xie, Z.; Feng, S.; Wang, P.; Zhang, L.; Ren, X.; Cui, L.; Zhai, T.; Chen, J.; Wang, Y.; Wang, X.; Sun, W.; Ye, J.; Han, P.; Klar, P. J.; Zhang, Y. Demonstration of a 3D Radar-Like SERS Sensor Micro- and Nanofabricated on an Optical Fiber. *Adv. Opt. Mater.* **2015**, *3*, 1232−1239.

(25) Dietrich, P. I.; Blaicher, M.; Reuter, I.; Billah, M.; Hoose, T.; Hofmann, A.; Caer, C.; Dangel, R.; Offrein, B.; Troppenz, U.; Moehrle, M.; Freude, W.; Koos, C. In situ 3D nanoprinting of free-form coupling elements for hybrid photonic integration. *Nat. Photonics* **2018**, *12*, 241−247.

(26) Gissibl, T.; Thiele, S.; Herkommer, A.; Giessen, H. Sub-micrometre accurate free-form optics by three-dimensional printing on single-mode fibres. *Nat. Commun.* **2016**, *7*, No. 11763.
(27) Gissibl, T.; Schmid, M.; Giessen, H. Spatial beam intensity shaping using phase masks on single-mode optical fibers fabricated by femtosecond direct laser writing. *Optica* **2016**, *3*, 448−451.
(28) Power, M.; Thompson, A. J.; Anastasova, S.; Yang, G.-Z. A Monolithic Force-Sensitive 3D Microgripper Fabricated on the Tip of an Optical Fiber Using 2-Photon Polymerization. *Small* **2018**, *14*, No. 1703964.
(29) Pagliano, S.; Marschner, D. E.; Maillard, D.; Ehrmann, N.; Stemme, G.; Braun, S.; Villanueva, L. G.; Niklaus, F. Micro 3D printing of a functional MEMS accelerometer. *Microsyst. Nanoeng.* **2022**, *8*, No. 105.
(30) Lao, Z.; Sun, R.; Jin, D.; Ren, Z.; Xin, C.; Zhang, Y.; Jiang, S.; Zhang, Y.; Zhang, L. Encryption/decryption and microtarget capturing by pH-driven Janus microstructures fabricated by the same femtosecond laser printing parameters. *Int. J. Extreme Manuf.* **2021**, *3*, No. 025001.
(31) Yu, H.; Ding, W.; Zhang, B. Y.; Gu, Z.; Gu, M. Three-Dimensional Direct Laser Writing of PEGda Hydrogel Microstructures with Low Threshold Power using a Green Laser Beam. *Light: Adv. Manuf.* **2021**, *2*, 31−38.
(32) Zou, M.; Liao, C.; Chen, Y.; Xu, L.; Tang, S.; Xu, G.; Ma, K.; Zhou, J.; Cai, Z.; Li, B.; Zhao, C.; Xu, Z.; Shen, Y.; Liu, S.; Wang, Y.; Gan, Z.; Wang, H.; Zhang, X.; Kasas, S.; Wang, Y. 3D printed fiber-optic nanomechanical bioprobe. *Int. J. Extreme Manuf.* **2023**, *5*, No. 015005.
(33) Xiong, C.; Zhou, J.; Liao, C.; Zhu, M.; Wang, Y.; Liu, S.; Li, C.; Zhang, Y.; Zhao, Y.; Gan, Z.; Venturelli, L.; Kasas, S.; Zhang, X.; Dietler, G.; Wang, Y. Fiber-Tip Polymer Microcantilever for Fast and Highly Sensitive Hydrogen Measurement. *ACS Appl. Mater. Interfaces* **2020**, *12*, 33163−33172.
(34) Liao, C.; Xiong, C.; Zhao, C.; Zou, M.; Zhao, C.; Li, B.; Ji, Z.; Cai, J.; Gan, Z.; Wang, C.; Wang, C. Design and realization of 3D printed fiber-tip microcantilever probes applied to hydrogen sensing. *Light: Adv. Manuf.* **2022**, *3*, No. 5.
(35) Li, C.; Liu, Y.; Lang, C.; Zhang, Y.; Qu, S. Femtosecond laser direct writing of a 3D microcantilever on the tip of an optical fiber sensor for on-chip optofluidic sensing. *Lab Chip* **2022**, *22*, 3734−3743.
(36) Tottori, S.; Zhang, L.; Qiu, F.; Krawczyk, K. K.; Franco-Obregón, A.; Nelson, B. J. Magnetic Helical Micromachines: Fabrication, Controlled Swimming, and Cargo Transport. *Adv. Mater.* **2012**, *24*, 811−816.
(37) Kim, S.; Qiu, F.; Kim, S.; Ghanbari, A.; Moon, C.; Zhang, L.; Nelson, B. J.; Choi, H. Fabrication and Characterization of Magnetic Microrobots for Three-Dimensional Cell Culture and Targeted Transportation. *Adv. Mater.* **2013**, *25*, 5863−5868.
(38) Zandrini, T.; Taniguchi, S.; Maruo, S. Magnetically Driven Micromachines Created by Two-Photon Microfabrication and Selective Electroless Magnetite Plating for Lab-on-a-Chip Applications. *Micromachines* **2017**, *8*, No. 35.
(39) Wang, W.-K.; Sun, Z.-B.; Zheng, M.-L.; Dong, X.-Z.; Zhao, Z.-S.; Duan, X.-M. Magnetic Nickel−Phosphorus/Polymer Composite and Remotely Driven Three-Dimensional Micromachine Fabricated by Nanoplating and Two-Photon Polymerization. *J. Phys. Chem. C* **2011**, *115*, 11275−11281.
(40) Liu, G.; Zhang, X.; Chen, X.; He, Y.; Cheng, L.; Huo, M.; Yin, J.; Hao, F.; Chen, S.; Wang, P.; Yi, S.; Wan, L.; Mao, Z.; Chen, Z.; Wang, X.; Cao, Z.; Lu, J. Additive manufacturing of structural materials. *Mater. Sci. Eng., R* **2021**, *145*, No. 100596.
(41) Xin, C.; Jin, D.; Li, R.; Wang, D.; Ren, Z.; Liu, B.; Chen, C.; Li, L.; Liu, S.; Xu, B.; Zhang, Y.; Hu, Y.; Li, J.; Zhang, L.; Wu, D.; Chu, J. Rapid and Multimaterial 4D Printing of Shape-Morphing Micromachines for Narrow Micronetworks Traversing. *Small* **2022**, *18*, No. 2202272.
(42) Fang, Y.-L.; Huang, Y.-H.; Kuo, C.-Y.; Chiang, C.-C. U-bend fiber optical sensor for magnetic field sensing. *Opt. Quantum Electron.* **2019**, *51*, No. 36.
(43) Tian, Y.; Lu, D.; Jiang, H.; Lin, X. Preparation of a novel ferrofluidic photoresist for two-photon photopolymerization technique. *J. Magn. Magn. Mater.* **2012**, *324*, 3291−3294.
(44) Xia, H.; Wang, J.; Tian, Y.; Chen, Q.-D.; Du, X.-B.; Zhang, Y.-L.; He, Y.; Sun, H.-B. Ferrofluids for Fabrication of Remotely Controllable Micro-Nanomachines by Two-Photon Polymerization. *Adv. Mater.* **2010**, *22*, 3204−3207.
(45) Shao, G.; Ware, H. O. T.; Huang, J.; Hai, R.; Li, L.; Sun, C. 3D printed magnetically-actuating micro-gripper operates in air and water. *Addit. Manuf.* **2021**, *38*, No. 101834.
(46) Sun, S.; Zeng, H.; Robinson, D. B.; Raoux, S.; Rice, P. M.; Wang, S. X.; Li, G. Monodisperse MFe2O4 (M = Fe, Co, Mn) Nanoparticles. *J. Am. Chem. Soc.* **2004**, *126*, 273−279.
(47) Ding, W.; Guo, Z.; Ruoff, R. S. Effect of cantilever nonlinearity in nanoscale tensile testing. *J. Appl. Phys.* **2007**, *101*, No. 034316.

https://doi.org/10.1021/acsphotonics.3c00347
ACS Photonics 2023, 10, 1916−1924